



MCM-41 supported quaternary ammonium ionic liquids as an effective heterogeneous catalyst for CO₂ cycloaddition reaction

Qing Lu¹ · Shougui Wang² · Cailin Ji¹ · Guanghui Chen¹ · Jipeng Dong¹ · Fei Gao¹

Accepted: 4 January 2024 / Published online: 18 February 2024

© The Author(s), under exclusive licence to Springer Science+Business Media, LLC, part of Springer Nature 2024

Abstract

Ionic liquid immobilization is an effective means for preparing metal-free heterogeneous catalysts for the CO₂ conversion. Herein, a series of quaternary ammonium ionic liquids functionalized MCM-41 heterogeneous catalysts, integrating hydrogen bond donors and nucleophilic ion sites, were prepared by a post-synthetic modification method for the CO₂ cycloaddition reaction. The physicochemical properties of the catalysts were analyzed by XRD, EA, SEM, TEM, BET, FT-IR, TGA, NMR and XPS. The results show that the quaternary ammonium ionic liquids are successfully immobilized onto the MCM-41 molecular sieves. The obtained catalysts maintain an excellent pore structure and have the good thermal stability. The effects of catalytic conditions on the catalytic performance, the recyclability of the catalysts and their generalizability to epoxide substrates were systematically investigated. In addition, the catalytic performance was evaluated for low concentrations of CO₂ (20% CO₂, 80% N₂). The synergy of multifunctional active sites makes the obtained materials exhibit the high catalytic activity without metals, co-catalysts and solvents. Furthermore, a possible mechanism for the conversion of CO₂ to cyclic carbonate catalyzed by the MCM-41-N/CH₃(1:3) was proposed.

Keywords CO₂ · Ionic liquids · Cycloaddition reaction · MCM-41 · Immobilization

1 Introduction

The greenhouse effect caused by the massive emission of greenhouse gases (GHGs) has attracted extensive concerns, and carbon dioxide (CO₂) accounts for approximately 60% of the total GHGs [1–3]. However, as a renewable, poison-free and cheap C1 resource, CO₂ is abundant in nature and can be used to produce various chemicals. Thus, the utilization of carbon dioxide resources can not only bring significant economic benefits, but also solve environmental problems [4, 5]. The reaction route of chemically transforming CO₂ with epoxides to prepare high-value-added chemical products cyclic carbonate has a low substrate raw material price and a 100% reaction atom utilization rate, following the concept of the circular economy and green chemistry [6,

7]. Since carbon dioxide is a stable molecule with the chemical inertness, it is important to develop rational and efficient catalysts for the carbon dioxide cycloaddition reaction.

At present, various homogeneous and heterogeneous catalytic systems, including metal oxides [8], organic bases [9], metal complexes [10], ionic liquids [11], porous organic polymers (POPs) [12] and metal–organic frameworks (MOFs) [13], have been developed for the CO₂ cycloaddition to prepare cyclic carbonates. Among them, metal functionalized catalysts exhibit the good catalytic activity for the CO₂ cycloaddition reactions. However, metal based catalysts have the disadvantages of the high cost, poor durability, susceptibility to gas poisoning, and are prone to the environmental pollution. Therefore, it is of great significance to create a series of metal-free environmentally friendly catalysts for CO₂ cycloaddition reactions. Ionic liquids have the advantages of the excellent solubility, adjustable acidity, simple preparation, low flammability, low toxicity, outstanding electrochemical and thermal stability, making them more advantageous in the field of catalysis [14–17]. Ionic liquids exhibit the excellent catalytic activity resulting from their nucleophilic halogen sites, and are considered promising catalysts to replace conventional metal-based catalysts for

✉ Fei Gao
feigao@tju.edu.cn

¹ College of Chemical Engineering, Qingdao University of Science and Technology, Qingdao 266042, China

² Department of Chemical Engineering, Qingdao University of Science and Technology (Gaomi Campus), Gaomi 261500, China

CO₂ cycloaddition reactions [18–21]. Among them, quaternary ammonium ionic liquids have the advantages of simple structure, easy preparation, adjustable acid–base active sites, and have been industrialized to catalyze the cycloaddition of CO₂ with epoxides to prepare cyclic carbonates. However, homogeneous ionic liquid catalysts have the high viscosity and are difficult to separate from the products, requiring the high energy consumption for the cumbersome catalyst recovery process [22–25]. Therefore, ionic liquid immobilization is an effective means to address these issues.

MCM-41 molecular sieve is widely used in the adsorption and catalysis due to its uniform mesoporous structure, structural stability, large specific surface area, easy preparation, and abundant silica hydroxyl groups [26–28]. The silica hydroxyl groups on the MCM-41 molecular sieves can graft ionic liquids through the chemical bonding, and the resulting ionic liquid immobilized catalysts have excellent pore structure, which can increase the effective contact area between ionic liquids and substrates, improving the mass transfer and enhancing the recoverability of the catalyst [29]. Moreover, hydrogen bond donors have been proven to effectively activate the ring opening of epoxides, promoting cycloaddition reactions [30, 31]. Dai et al. [19] prepared a series of HBDs functionalized phosphine-based ionic liquids (FPBILs), and the hydrogen bond donors –COOH, –NH₂, and –OH groups in FPBILs could activate the ring-opening of epoxides, and the halogen anions could nucleophilically attack epoxides, enabling the prepared FPBILs catalyst to catalyze CO₂ conversion at the conditions of solvent-free and co-catalyst-free. Peng et al. [23] synthesized six polyhydroxylated quaternary ammonium ionic liquids as multifunctional catalysts for catalyzing CO₂ cycloaddition reactions. The synergistic interaction of hydroxyl groups and halogen anions can effectively activate the epoxides, which enables this catalyst system to catalyze the cycloaddition reaction even under the atmospheric pressure. Jentys et al. [32] confirmed that there are abundant silicon hydroxyl groups on the MCM-41 molecular sieve through the infrared spectroscopy, which can serve as hydrogen bond donors to assist halogen ions in ionic liquids in promoting the epoxide ring opening. Inspired by the pioneering works, the incorporation of task-specific ionic liquids into MCM-41 is a prospective strategy to construct metal-free heterogeneous catalyst for the CO₂ conversion to cyclic carbonates.

Herein, a series of MCM-41 immobilized quaternary ammonium ionic liquid catalysts were constructed by a post-synthesis modification method for efficiently catalyzing the CO₂ cycloaddition reaction. The obtained catalysts maintain a good pore structure, and the synergy of multifunctional active sites enable the resulting metal-free materials to exhibit a high catalytic activity under cocatalyst-free and solvent-free reaction conditions. In addition, the catalysts are recyclable with the outstanding versatility for various

epoxides. The catalytic performance in cycloaddition reaction still achieves high yields at low carbon dioxide concentrations. Furthermore, a feasible reaction mechanism for the MCM-41-N/CH₃(1:3) was also proposed.

2 Experimental

2.1 Materials

N₂ (99.999%) and CO₂ (99.999%) were purchased by Dehai Gas Co., Ltd. The MCM-41 (H-type, All-silica) was provided by Tianjin Nankai Catalyst Plant. Styrene oxide (SO), propylene oxide (PO), cyclohexene oxide (CO), epichlorohydrin (ECH), allyl glycidyl ether (AGE), 1,2-butylene oxide (BO), 1,4-butanediol diglycidyl ether (BDE), 1,6-hexanediol diglycidyl ether (HDK), diethyleneglykol-diglycidylether (DEDG), biphenyl, toluene, methylene chloride, anhydrous ethanol, n-butyl bromide, 1-bromobutyric acid, 3-aminopropyltrimethoxysilane (APTS), ethyl acetate and 1,2-dibromobutane were purchased from Aladdin Chemical Co., Ltd.

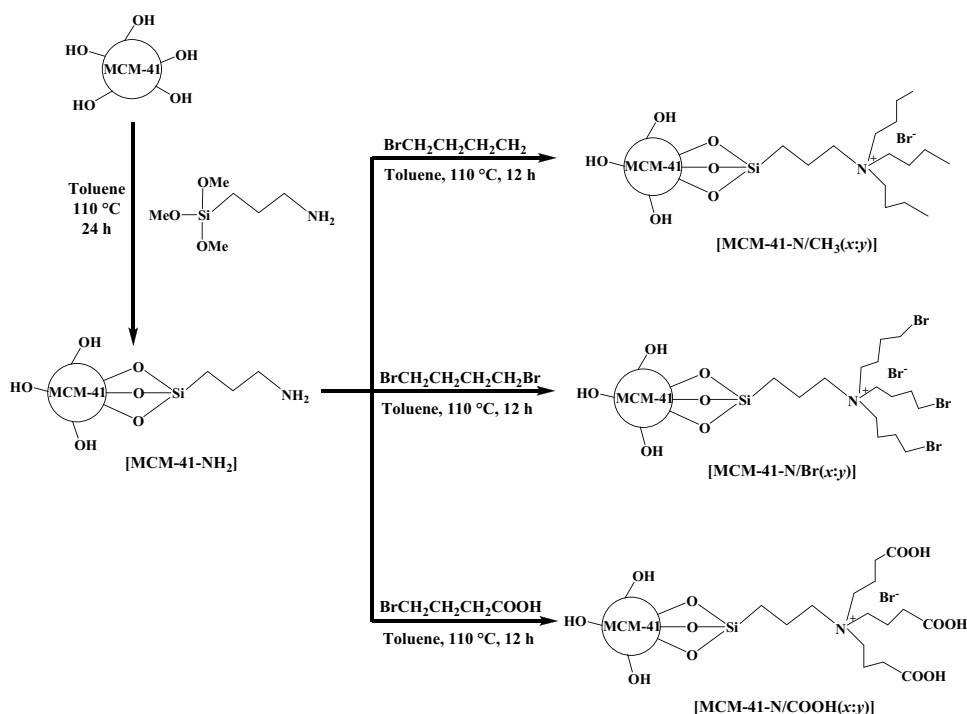
2.2 Catalyst synthesis

In a typical run, 5.44 mmol of APTS and 2.00 g of dried MCM-41 molecular sieves (120 °C for 4 h) were added into 50 ml of dry toluene. After the reaction at 110 °C with the continuous stirring for 24 h under N₂ atmosphere, the solids were collected and washed with methylene chloride and anhydrous ethanol, and then dried at 70 °C for 12 h. The obtained sample was named as MCM-41-NH₂. Subsequently, MCM-41-NH₂ samples were placed into the round-bottomed flask with varying amounts of n-butyl bromide, and 50 ml of dry toluene was added. The mixture was refluxed at 110 °C for 24 h under the N₂ atmosphere. After that, a series of quaternary ammonium ionic liquids functionalized MCM-41 samples were obtained, and denoted as MCM-41-N/CH₃(x:y), where *x* is the amount of APTS and *y* is the amount of n-butyl bromide. To investigate the catalytic performance of quaternary ionic liquids functionalized MCM-41 catalysts with different end groups of alkyl compounds, a series of MCM-41-N/Br(x:y) and MCM-41-N/COOH(x:y) catalysts were synthesized by substituting n-butyl bromide with 1-bromobutyric acid and 1,2-dibromobutane, respectively according to the aforementioned steps, and the synthetic routes are shown in Scheme 1.

2.3 Sample characterization

The structural properties for MCM-41 molecular sieves and MCM-41 functionalized with ionic liquids were analyzed using a D-MAX 2500/PC X-ray diffractometer. The low-angle scanning range is 2θ = 1°–10° and the wide-angle

Scheme 1 Schematic synthesis of MCM-41-N/X(x:y) (X = CH₃, Br or COOH)



scanning range is $2\theta = 5^\circ\text{--}80^\circ$. The changes in functional groups of MCM-41 before and after the ionic liquids immobilization were detected using a Nicolet iS10 FTIR spectrometer, and the FT-IR curves of the samples were determined in the range of $400\text{--}4000\text{ cm}^{-1}$. The mass percentages of the elements N, H and C in the samples were determined using a Vario EL III model elemental analyzer (EA). An TGA/DSC 1 thermogravimetric analyzer (TGA) was used to determine the variation of sample mass with the temperature in N₂ atmosphere. The textural properties were measured by using the ASAP 2460 automatic physical adsorption instrument to measuring the N₂ adsorption/desorption isotherms at 77 K. The microstructures of the samples were observed using the Sigma 500 scanning electron microscope (SEM) and HT7800 transmission electron microscope (TEM). An ESCALAB 250Xi X-ray photoelectron spectrometer (XPS, Thermo Fisher Scientific) and a Varian Infinity Plus 400 NMR spectrometer were used to examine chemical compositions of the samples.

2.4 Cycloaddition reactions and analytical methods

The cycloaddition reactions of CO₂ with epoxides were conducted in an autoclave (25 ml). Typically, a given amount of PO and catalyst was added into the autoclave, and CO₂ was pressed to a specified pressure. Subsequently, the reactor was sealed and heated to the given temperature using the oil bath. After reacting under stirring for a period of time, the reactor was cooled and depressurized slowly. The solid phase was gathered by the centrifugation, and the collected

liquid phase was analyzed by GC and GC–MS using ethyl acetate as the solvent and biphenyl as the internal standard. In the cyclic stability test, the recovered catalyst was washed repeatedly with ethyl acetate then dried for 6 h at 70 °C for the next reaction.

3 Results and discussion

3.1 Catalyst characterizations

Figure 1 shows the low and wide angle X-ray diffraction patterns of MCM-41 before and after the functionalization. It can be observed that MCM-41 molecular sieve has two weak peaks at $2\theta = 4.4^\circ$ and 3.8° and an obvious diffraction peak at $2\theta = 2.2^\circ$, belonging to typical (200), (110) and (100) planes for the MCM-41 molecular sieve, respectively, showing the existence orthocrystalline arrangement of hexagonal mesopores [33]. In addition, the MCM-41 molecular sieves retain the obvious characteristic peaks after immobilizing the three quaternary ammonium ionic liquids, showing that the crystal structure of the immobilized samples does not change and still retains the mesoporous structure. Additionally, it can be seen that the intensity of the (100), (110) and (200) peaks on the planes of the immobilized samples is weakened or even disappeared, suggesting that the quaternary ionic liquids do not simply attach onto the external surface of the MCM-41 molecular sieves but enter the pores, which has some effect on the ordering of the MCM-41 pores

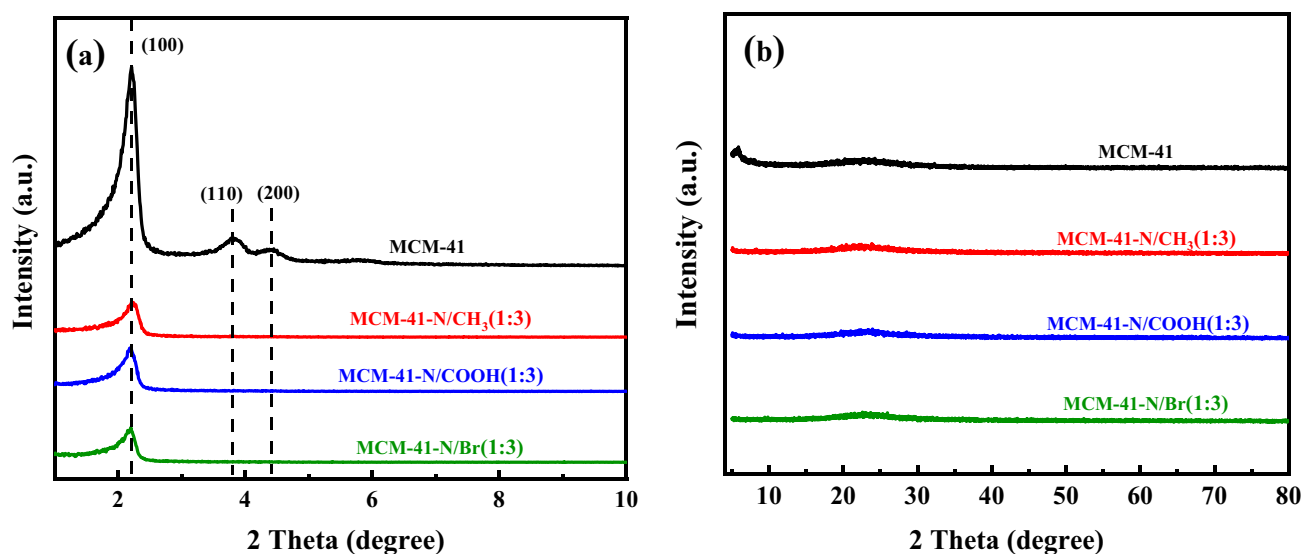


Fig. 1 XRD patterns of MCM-41 before and after the functionalization: **a** low angle and **b** wide angle

Table 1 Elemental analysis of MCM-41-NH₂ and MCM-41 immobilized ionic liquids samples

Samples	C (wt%)	H (wt%)	N (wt%)
MCM-41-NH ₂	7.98	2.39	2.76
MCM-41-N/COOH(1:3)	10.52	2.58	2.41
MCM-41-N/Br(1:3)	10.02	2.18	2.30
MCM-41-N/CH ₃ (1:1)	10.10	2.47	2.45
MCM-41-N/CH ₃ (1:2)	10.85	2.30	2.53
MCM-41-N/CH ₃ (1:3)	11.24	2.67	2.42
MCM-41-N/CH ₃ (1:4)	11.39	2.43	2.43

[34]. The results indicate that the quaternary ionic liquids are successfully introduced into the MCM-41 pores.

The contents of elements N, H and C in the intermediate (MCM-41-NH₂) and the immobilized catalysts were determined by the elemental analysis, and the data are listed in Table 1. The N elements were detected in the MCM-41-NH₂ intermediates and the quaternary ammonium ionic liquids immobilized catalysts, which indicates that the APTS is successfully immobilized onto the surfaces of MCM-41 molecular sieve. Furthermore, compared to the MCM-41-NH₂ intermediate, the contents of H and C elements in the samples MCM-41-N/Br(1:3), MCM-41-N/COOH(1:3) and MCM-41-N/CH₃(1:3) are higher, indicating a successful connection of alkyl compounds to APTS, suggesting the successful functionalization of ionic liquids onto molecular sieves surfaces.

Figure 2 demonstrates the FT-IR spectra of MCM-41, intermediate (MCM-41-NH₂), immobilized catalysts and pure quaternary ammonium salt ionic liquid tetrabutylammonium bromide (Bu₄NBr). In the FT-IR spectra

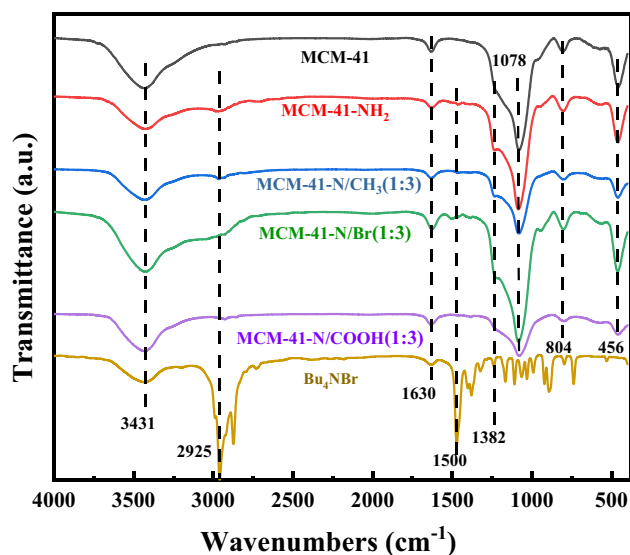


Fig. 2 FT-IR spectra of Bu₄NBr, MCM-41 with and without the functionalization

of MCM-41 molecular sieve, the peaks at 3431 cm⁻¹ and 1630 cm⁻¹ correspond to the stretching vibration of -OH groups on the surface of MCM-41 molecular sieve and physically adsorbed water, respectively [35]. The vibrational peak at 456 cm⁻¹ belongs to the silicon-oxygen bonds, the peak at 1078 cm⁻¹ is symmetric stretching vibration peak of silicon-oxygen-silicon bonds, and the peak at 804 cm⁻¹ is asymmetric stretching vibration peak of silicon-oxygen-silicon bonds [36]. After the immobilization with the silane coupling agent APTS and quaternary ammonium ionic liquid, all adsorption peaks of MCM-41 were also detected, which indicates that the fundamental structure of MCM-41

molecular sieves are retained in all the composites. The characteristic absorption peak near 2925 cm^{-1} in the FT-IR spectrum of MCM-41-NH₂ is the stretching vibration peak of the C–H group, which slightly shifts after grafting the alkyl compounds, which may be due to the increase in the C–H groups, enhancing the interaction with other molecules, affecting its vibrational frequency [37]. In addition, in the samples MCM-41-NH₂ and functionalized ionic liquid catalysts, the absorption peaks around $1382\text{--}1502\text{ cm}^{-1}$ are the C–N bond stretching vibration peaks, suggesting that APTS is successfully immobilized onto MCM-41. Moreover, the functionalized ionic liquid catalysts show the similar position of C–N absorption peaks with Bu₄NBr, indicating that the quaternary ammonium ionic liquids are successfully immobilized onto MCM-41 molecular sieves.

The N₂ adsorption/desorption isotherms and pore size distribution curves of MCM-41 before and after the immobilization are shown in Fig. 3, and Table 2 presents the total pore volume, average pore size and specific surface area. From Fig. 3a, all samples exhibit typical IV representative adsorption isotherms, which illustrates that MCM-41 molecular sieves maintain mesoporous properties after immobilizing APTS and quaternary ammonium ionic liquids. As shown in Table 2, MCM-41 molecular sieves have excellent pore diameter, pore volume and large specific surface area, which facilitates the immobilization of ionic liquids. The pore parameters of MCM-41 molecular sieves are decreased after the amine functionalization and quaternary ammonium ionic liquid immobilization, which is attributed to the fact that APTS and quaternary ammonium ionic liquid occupy the partial surface area and pore volume of MCM-41 molecular sieves, suggesting that ionic liquids are successfully integrated onto the surface of MCM-41. In addition, the pore size distribution curves (Fig. 3b) further confirm

Table 2 Textural properties of MCM-41 before and after the functionalization

Samples	BET surface area ($\text{m}^2\text{ g}^{-1}$)	Total pore volume ($\text{cm}^3\text{ g}^{-1}$)	Average pore diameter (nm)
MCM-41	1025	0.921	3.169
MCM-41-NH ₂	906.3	0.726	3.100
MCM-41-N/CH ₃ (1:3)	610	0.343	2.510
MCM-41-N/Br(1:3)	697	0.380	2.473
MCM-41-N/COOH(1:3)	865	0.436	2.443

the presence of mesopores and the partial blockage of pores after the ionic liquid functionalization. The mesoporous structure in catalysts is conducive to the sufficient contact between active sites and substrates.

The morphologies of MCM-41 molecular sieves and the immobilized quaternary ammonium ionic liquid catalysts were analyzed by SEM and TEM. From Fig. 4a, it can be observed that MCM-41 molecular sieve consists of fragments with different sizes. The SEM images of the immobilized quaternary ammonium ionic liquid catalysts samples (Fig. 4b–d) show that the overall morphology of MCM-41 molecular sieve has no obvious change after the modification, while the surface of the particles becomes flatter. From the TEM images of MCM-41 before and after the ionic liquid immobilization (Fig. 4e–h), all the samples show the uniform and ordered pores pore channels, suggesting that the MCM-41 support is intact and maintains a uniform pore structure after grafting ionic liquids. In addition, it can be observed that the pores of immobilized ionic liquid catalysts become darker compared with the parent MCM-41, indicating a successful confinement of ionic liquids into

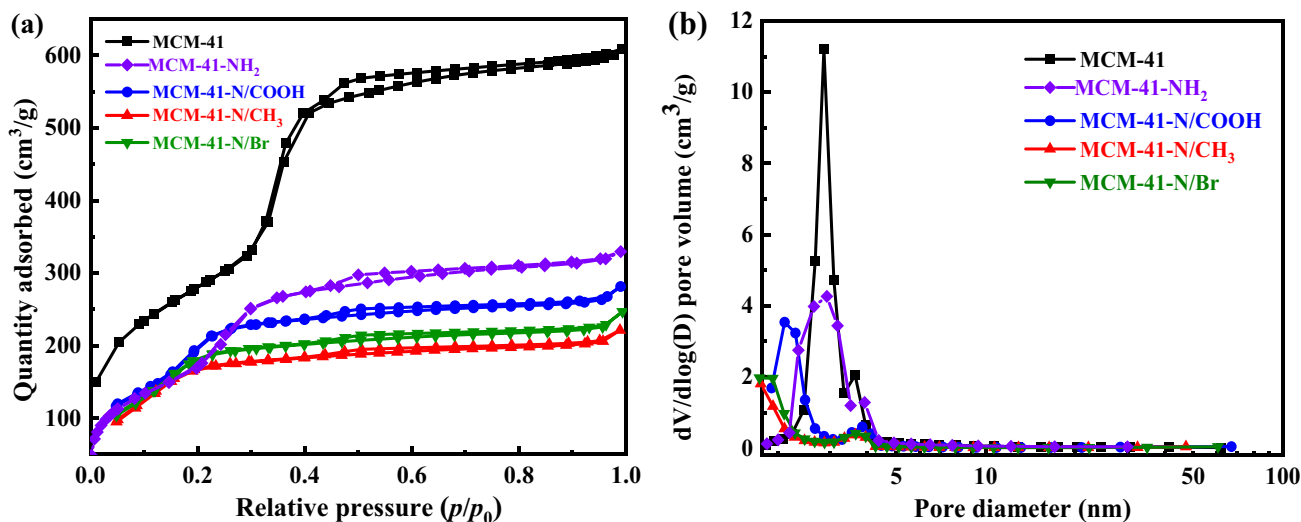


Fig. 3 a N₂ adsorption and desorption isotherms at 77 K and b pore size distribution curves of MCM-41 before and after the functionalization

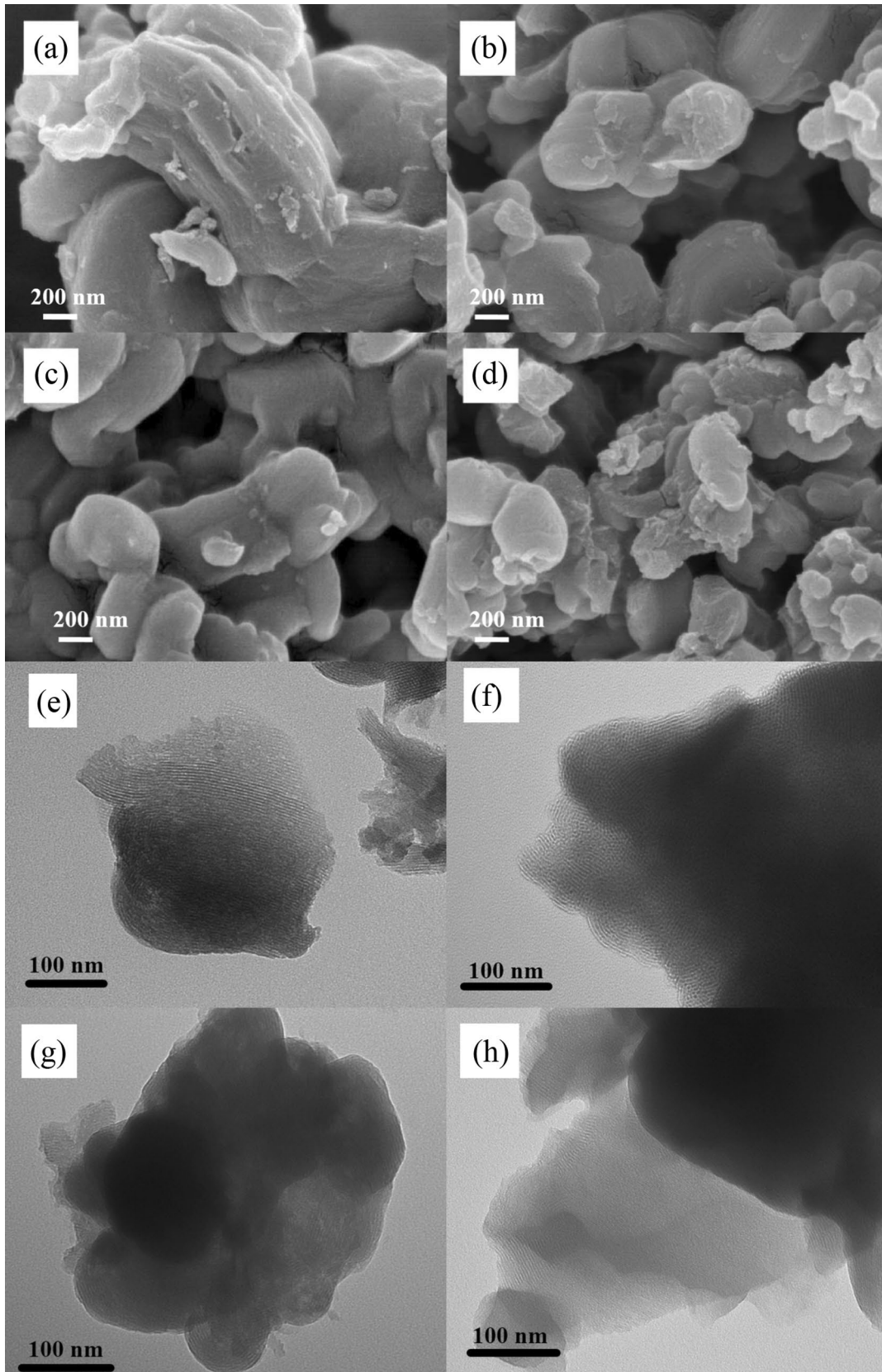


Fig. 4 SEM images of **a** MCM-41, **b** MCM-41-N/CH₃(1:3), **c** MCM-41-N/Br(1:3) and **d** MCM-41-N/COOH(1:3); TEM images of **e** MCM-41, **f** MCM-41-N/CH₃(1:3), **g** MCM-41-N/Br(1:3) and **h** MCM-41-N/COOH(1:3)

the mesopores of MCM-41. Combined with FT-IR, EA and XRD analysis results, it can be confirmed that APTS and quaternary ammonium ionic liquids are successfully introduced MCM-41 molecular sieves without destroying the MCM-41 molecular sieves, and the presence of silane coupling agents make the inter-particles more compact.

Figure 5 shows the thermogravimetric analysis of the MCM-41 and three quaternary ammonium ionic liquid immobilized catalysts. It can be seen that the weight of all the samples is lost by about 2% from 30 to 110 °C, which is due to the removal of other gas components and water in the samples. When further increasing the temperature to 600 °C, the weight of MCM-41 molecular sieve is almost constant, and the quaternary ammonium ionic liquid immobilized

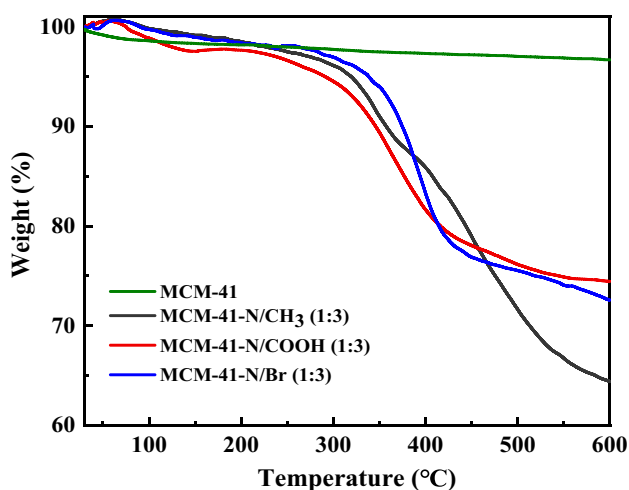


Fig. 5 TGA curves of MCM-41 and quaternary ionic liquid functionalized catalysts

catalysts show a good stability in the range of 110–300 °C. Generally, the reaction temperature of the CO₂ cycloaddition is within 150 °C, which indicates that the prepared quaternary ammonium ionic liquid catalysts exhibit the excellent structural stability.

Figure 6a shows the ¹³C-MAS-NMR of MCM-41-N/CH₃(1:3), MCM-41-N/Br(1:3), and MCM-41-N/COOH(1:3). For the samples MCM-41-N/CH₃(1:3) and MCM-41-N/Br(1:3), the signals of all the methylene and terminal carbon atoms on the branched chain connected to the quaternary ammonium nitrogen are detected at around 13–60 ppm [38, 39]. For the sample MCM-41-N/COOH(1:3), in addition to the methylene signals, the signal at 169 ppm is ascribed to the C=O carbon atoms in the carboxyl groups [11]. Figure 6b shows the ²⁹Si-MAS-NMR spectrogram of MCM-41-N/CH₃(1:3). The signals at –110 ppm and –105 ppm belong to siloxane Q⁴ [Si(OSi)₄] and Q³ [Si(OSi)₃(OH)] in MCM-41, respectively, and the signals at –71 ppm and –62 ppm belong to the organic siloxane T³ [RSi(OSi)₃] and T² [RSi(OSi)₂(OH)], respectively [40]. The NMR results confirm the successful connection of quaternary ammonium ionic liquids with MCM-41.

The chemical composition and elemental valence states of the prepared MCM-41-N/CH₃(1:3) were further analyzed by XPS. As shown in Fig. 7a, C, N, O, Br and Si elements were detected in the survey scan spectrum of MCM-41-N/CH₃(1:3), indicating the successful modification of MCM-41. As shown in Fig. 7b, the N 1s signal of MCM-41-N/CH₃(1:3) was deconvoluted into two peaks at 400.5 eV and 398.0 eV, representing the C–N⁺ bond (quaternary ammonium) and C–N bond (tertiary amine), respectively [41]. Based on the peak intensity of N 1s signal, most of the nitrogen atoms are in the form of quaternary ammonium

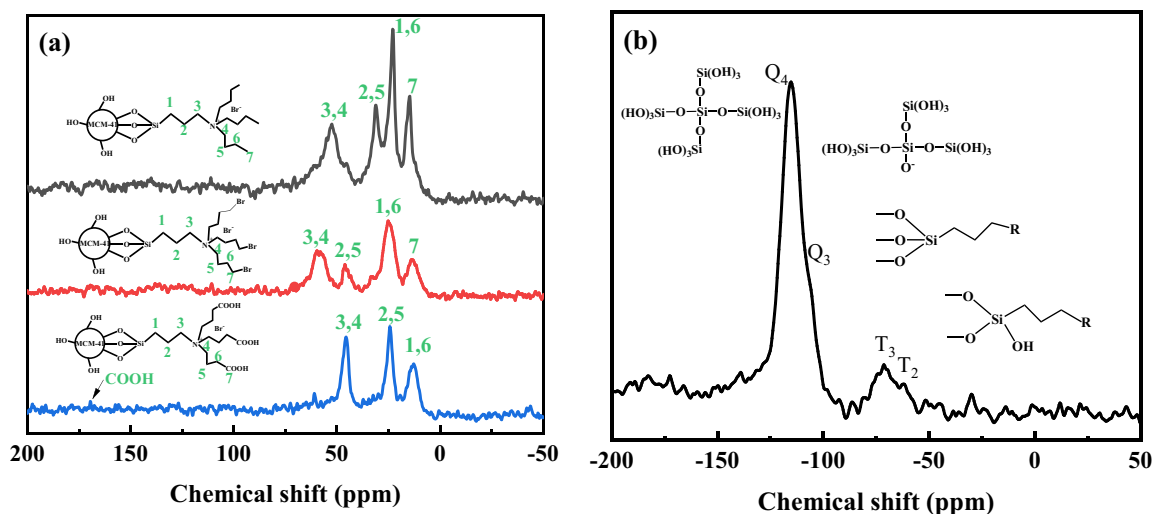


Fig. 6 **a** ¹³C MAS-NMR of MCM-41-N/CH₃(1:3), MCM-41-N/Br(1:3) and MCM-41-N/COOH(1:3) and **b** ²⁹Si-MAS-NMR of MCM-41-N/CH₃(1:3)

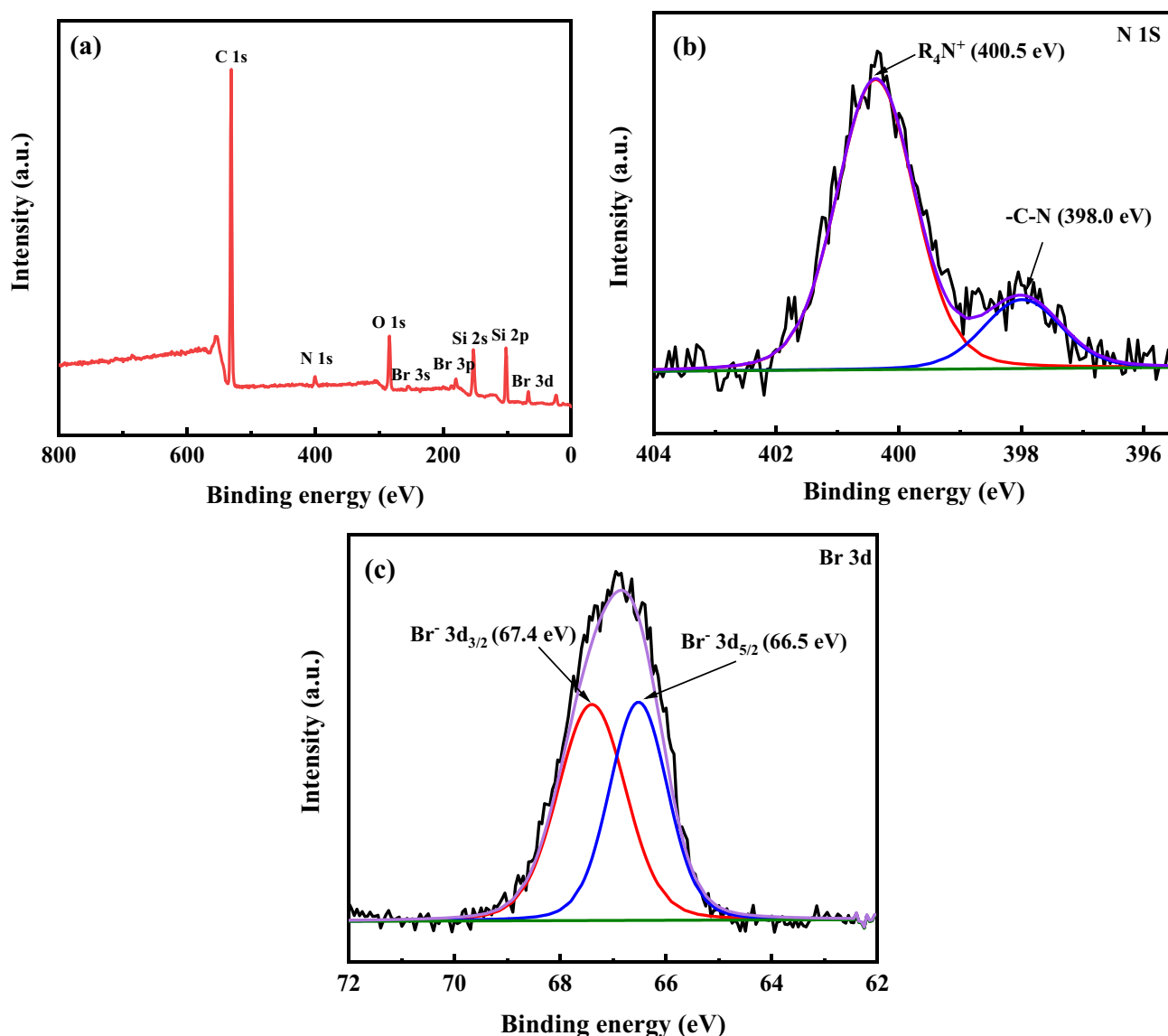


Fig. 7 a Survey scan, b N 1s, and c Br 3d XPS spectra of MCM-41-N/CH₃(1:3)

salts. As shown in Fig. 7c, the Br 3d signal was deconvoluted into two peaks at 67.4 eV and 66.5 eV, corresponding to Br⁻ 3d_{3/2} and Br⁻ 3d_{5/2}, respectively [25], indicating the existence of nucleophilic active sites free Br⁻ anions in the catalyst. The XPS analysis further confirms that the quaternary ammonium salt ionic liquid is successfully integrated onto the surfaces of MCM-41 molecular sieves.

3.2 Catalyst performance for cycloaddition reactions

3.2.1 Catalyst screening

The catalytic properties of MCM-41 molecular sieves before and after the modification were tested for the CO₂

cycloaddition using PO as the model substrate, and the results are summarized in Table 3. From Table 3, MCM-41 molecular sieves have no activity for the CO₂ cycloaddition reaction. With the introduction of APTS, the MCM-41-NH₂ intermediate have the low activity, and the yield of PC is only 47.6% with a selectivity of 92.5%. After immobilizing quaternary ammonium ionic liquids, the catalytic performance is greatly improved, and the yield of PC increases with the increase in the proportion of alkyl compounds in MCM-41-N/COOH(*x*:*y*) and MCM-41-N/Br(*x*:*y*) catalysts. This is due to the increase in ionic liquid active sites, which facilitates the activation of the epoxide, promoting the cycloaddition reaction. For MCM-41-N/CH₃(*x*:*y*) catalysts, the PC yield gradually increases to 92.5% when the ratio of APTS to alkyl compounds is increased from 1:1 to 1:3,

Table 3 Catalytic activities of MCM-41 before and after the modification for the cycloaddition reaction

Catalyst	Yield (%) ^a	Selectivity (%) ^a
MCM-41	–	–
MCM-41-NH ₂	47.6	92.5
Bu ₄ NBr	53.43	96.6
MCM-41-N/COOH(1:1)	79.3	96.7
MCM-41-N/COOH(1:2)	84.5	96.8
MCM-41-N/COOH(1:3)	85.0	96.9
MCM-41-N/COOH(1:4)	90.2	97.0
MCM-41-N/Br(1:1)	82.7	97.4
MCM-41-N/Br(1:2)	85.7	97.7
MCM-41-N/Br(1:3)	90.2	95.8
MCM-41-N/Br(1:4)	90.5	97.9
MCM-41-N/CH ₃ (1:1)	85.2	95.6
MCM-41-N/CH ₃ (1:2)	88.8	95.8
MCM-41-N/CH ₃ (1:3)	92.5	96.6
MCM-41-N/CH ₃ (1:4)	90.6	95.5

Reaction conditions: PO 1.0 g (17 mmol), catalyst addition amount 150 mg, initial pressure 2.0 MPa, reaction temperature 140 °C, reaction time 3 h

^aDetermined by GC analysis

and when further increasing this ratio to 1:4, the PC yield decreases. According to the results of elemental analysis, the ionic liquid content in MCM-41-N/CH₃(1:4) is higher than that in MCM-41-N/CH₃(1:3), so the decrease in the yield of MCM-41-N/CH₃(1:4) might be due to the introduction of excessive n-butyl bromide, leading to the blockage of part of the pores. In addition, it can be found that at the same ratio of APTS to alkyl compounds, the PC yield of MCM-41-N/CH₃ is better than those of MCM-41-N/Br and MCM-41-N/COOH, and the PC selectivities are all above 95.0%. The above results indicate that the catalytic activity of MCM-41-N/CH₃(1:3) is superior to other catalysts, which may be due to the abundant hydroxyl hydrogen bond donors in MCM-41 molecular sieves, and the introduction of more hydrogen-bonding donors have little effect on the CO₂ cycloaddition catalytic activity. In addition, the pure quaternary ammonium salt ionic liquid Bu₄NBr shows a catalytic activity of 64% PC yield, which is significantly lower than that of ionic liquid functionalized MCM-41 catalysts, highlighting the roles of abundant pore structures for the CO₂ enrichment and the substrate diffusion in the catalytic process.

3.2.2 Effect of reaction parameter

The influence of reaction conditions on the catalytic performance was further investigated for the catalyst MCM-41-N/CH₃(1:3). Figure 8a illustrates the changes in the catalytic activity with the reaction temperature. The yield

of PC increases from 66.9 to 92.5% when the temperature is increased from 100 to 140 °C, and decreases slightly when the reaction temperature continues to increase to 150 °C. This is due to the fact that within a certain temperature range, molecules gain energy by increasing the temperature, which increases the probability of collision, thereby improving the yield. Excessive temperature will promote the occurrence of side reactions, resulting in a slight decrease in the PC yield [42]. The catalyst MCM-41-N/CH₃(1:3) shows a high PC selectivity of above 95.0% at different reaction temperatures.

The effect of the reaction pressure on the yield and selectivity of PC is shown in Fig. 8b. The selectivity of PC is about 95.0% at different pressures. The yield of PC increases from 71.4 to 92.5% with increasing the pressure from 1.0 to 2.0 MPa. This is attributable to the increase in the CO₂ concentration as the reaction pressure increases, which accelerates the rate of the cyclization reaction. When further increasing the pressure to 3.0 MPa, the PC yield remains almost unchanged owing to the given amount of PO in the reactor, and increasing CO₂ concentration has little effect on the reaction while the reaction rate is maximized [43].

The influence of the reaction time on the catalytic cycloaddition performance of the catalyst is shown in Fig. 8c. From Fig. 8c, the yield of PC gradually increases from 74.9 to 92.5% when the reaction time is increased from 1 to 3 h. When the reaction time is further increased to 4 h, the PC yield has no obvious change. The catalyst MCM-41-N/CH₃(1:3) shows a high PC selectivity in this temperature range, which is higher than 95.0%. However, as the time prolongs, the yield and selectivity of PC begin to decrease, mainly attributed to a decrease in the concentration of PO and CO₂, and the inability to separate PC in a timely manner when the reaction substrate is completely converted. At a certain temperature and pressure, PC may undergo side reactions such as the polymerization or isomerization, resulting in a large number of by-products and a slight decrease for the target product yield.

Figure 8d shows the effect of the catalyst dosage on the catalytic performance of MCM-41-N/CH₃(1:3). It can be seen that when the dosage is increased from 50 to 150 mg, the catalyst active site increases, resulting in a changes in yield of PC from 71.6 to 92.5%. When further increasing the catalyst dosage, both the yield and selectivity show a decreasing trend. This may be attributed to that the excessive catalyst dosage will hinder the surface quality and heat transfer of some catalysts and block the active sites, reducing the catalytic efficiency, thereby resulting in a corresponding decrease in PC yield [44]. In addition, the selectivity of PC is basically the same at different catalyst dosages, which is maintained at about 96.0%.

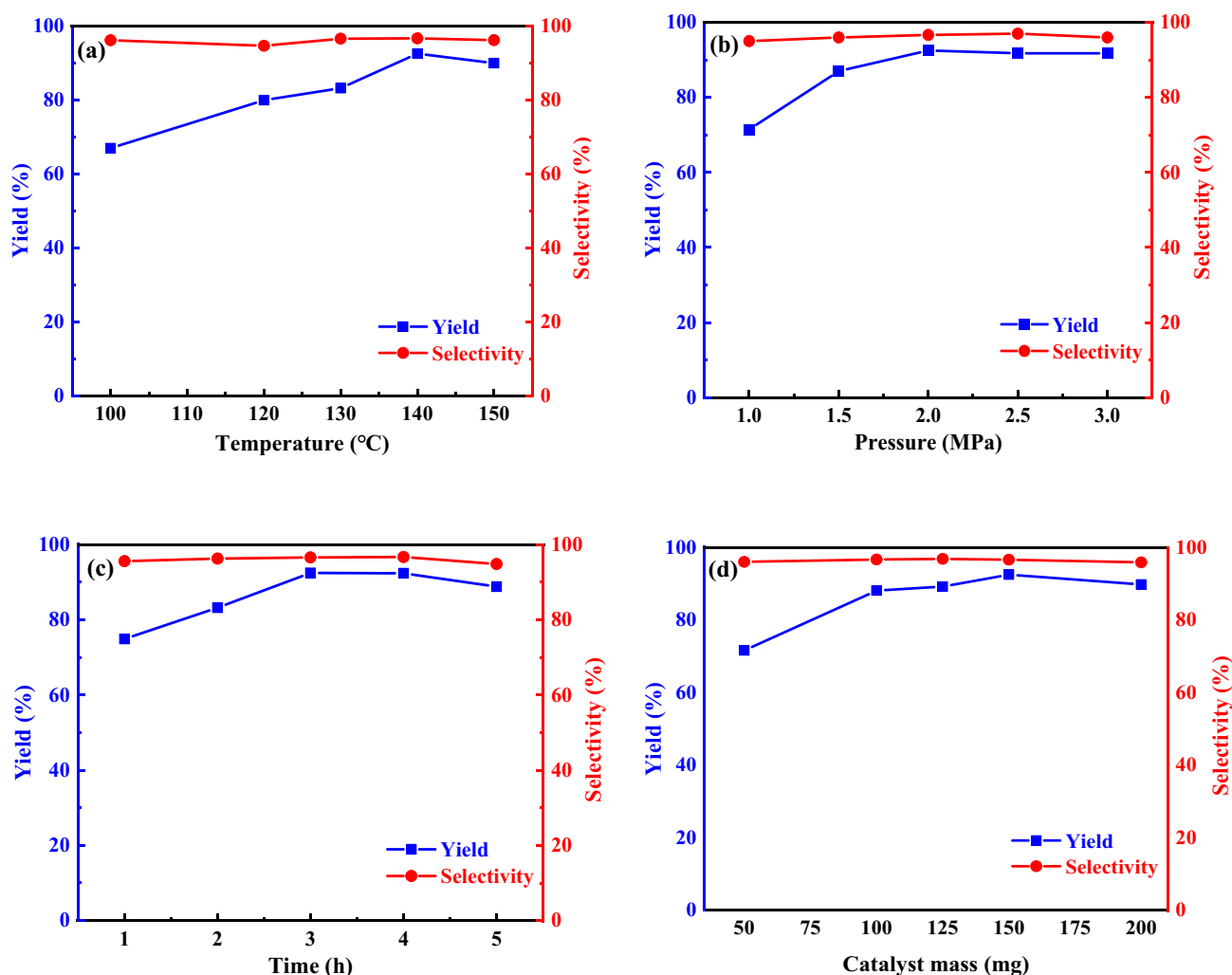


Fig. 8 Influences of reaction conditions on the catalytic activity for the cycloaddition reaction of MCM-41-N/CH₃: **a** temperature (PO 17 mmol, catalyst 150 mg, 3 h, CO₂ 2.0 MPa), **b** CO₂ pressure (PO

17 mmol, catalyst 150 mg, 3 h, 140 °C), **c** time (PO 17 mmol, catalyst 150 mg, CO₂ 2.0 MPa, 140 °C), and **d** catalyst dosage (PO 17 mmol, 3 h, CO₂ 2.0 MPa, 140 °C)

3.2.3 Effect of CO₂ concentration

The actual concentration of CO₂ in the exhaust gas is relatively low, especially in the exhaust gas generated by the combustion of fossil fuels, which is about 20%, requiring a catalyst with the good catalytic activity to achieve the cycloaddition of CO₂ and epoxides at low CO₂ concentrations. To verify the availability of the prepared MCM-41-N/CH₃(1:3) catalyst at low concentrations of CO₂, the cycloaddition reaction between CO₂ and epoxide at low CO₂ concentrations was conducted. The pressure was 2.0 MPa for all the experiments, and the CO₂ concentrations were adjusted by adjusting the amounts of N₂ and CO₂. The added amount of PO was 10 mmol and the volume of the reactor was chosen to be 50 ml to ensure the CO₂ sufficient. As shown in Table 4, the yield of PC decreases with the reduction in the CO₂ concentration, and when the concentration

of CO₂ is 50%, the yield of PC is 91.0%, only 1.5% lower than that when using pure CO₂. When the concentration of CO₂ is reduced to 20%, the yield of PC decreases to 78.8%. Moreover, the concentration of CO₂ has almost no effect on the selectivity of PC, which is higher than 96.0%. The above results show that the MCM-41-N/CH₃(1:3) has the excellent catalytic activity for the dilute CO₂ conversion to cyclic carbonates.

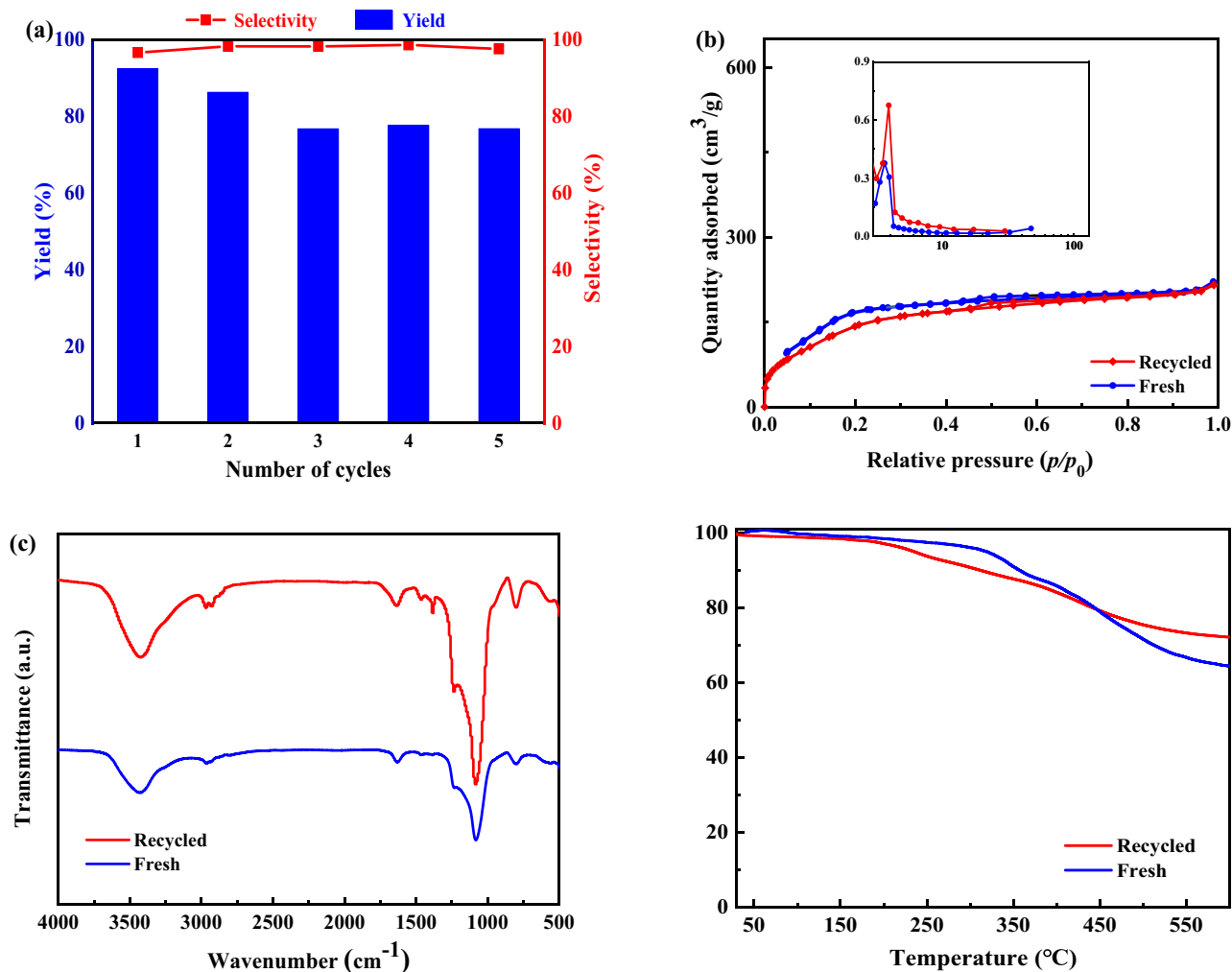
3.3 Reusability test

The recoverability of the MCM-41-N/CH₃(1:3) catalyst was evaluated under optimal conditions by the five consecutive reaction/regeneration cycles. As shown in Fig. 9, the PC yield decreases from 92.5 to 76.8% after first three cycles, which may be attributed to the unstable connection of a small portion of the quaternary ammonium ionic liquid immobilized on the

Table 4 Catalytic activity of MCM-41-N/CH₃(1:3) for low concentration of CO₂

CO ₂ mole fraction (%)	Temperature (°C)	Pressure (MPa)	Time (h)	Yield ^a (%)	Selectivity ^a (%)
99.9999	140	2.0	3	92.5	96.6
50	140	2.0	3	91.0	96.9
40	140	2.0	3	89.9	96.8
30	140	2.0	3	88.1	96.0
20	140	2.0	3	78.8	96.5

Reaction conditions: PO 1.0 g (17 mmol), catalyst addition amount 150 mg

^aDetermined by GC analysis**Fig. 9** a Effect of number of cycles on MCM-41-N/CH₃(1:3) catalytic performance for CO₂ cycloaddition. (Catalytic conditions: PO 1.0 g (17 mmol), 3 h, 2.0 MPa, 150 mg, 140 °C); b N₂ adsorption/desorp-tion isotherms and pore distribution, c FT-IR spectra, and d TGA curves of fresh and recycled MCM-41-N/CH₃(1:3)

catalysts, resulting in the loss of active components. The PC yields remains almost unchanged in the last two cycles. In the five cycles, the selectivity of PC remains basically unchanged. In addition, the recovered MCM-41-N/CH₃(1:3) was further characterized by the N₂ adsorption–desorption test, FT-IR and

TGA. The recovered sample exhibits the similar pore structure characteristics (Fig. 9b), functional groups (Fig. 9c) and thermogravimetric behavior to the fresh catalyst, indicating the well maintenance of physicochemical properties of MCM-41-N/CH₃(1:3) after the catalytic reaction. Furthermore, in

order to evaluate the heterogeneous nature of the prepared catalyst, the leaching test was conducted. After 1 h of the catalytic reaction, the MCM-41-N/CH₃(1:3) catalyst was removed by the filtration, and the filtrate was further reacted at the same reaction conditions for another 4 h without the catalyst. After removing the catalyst, the yield of PC barely increases from 75 to 77%, indicating the heterogeneity and good stability of the MCM-41-N/CH₃(1:3) catalyst. The above results show that the MCM-41-N/CH₃(1:3) catalyst possess the excellent recoverability and potential for the industrial application.

3.4 Catalytic properties of other epoxy substrates

Table 5 shows the catalytic activity of catalyst MCM-41-N/CH₃(1:3) for different epoxides. Evidently, the catalyst MCM-41-N/CH₃(1:3) has excellent catalytic performance for the mono-epoxides (entries 1–5, PO, AGE, BO, ECH, SO) and di-epoxides (entries 6–8 DEDG, DLD and HDK), and all the epoxides can be converted to the corresponding cyclic carbonates with yields of higher than 90%. For cyclohexene oxide (CO) (entry 9), the catalytic activity is lower with the yield and selectivity of the target product of 22.9% and 67.7%, respectively. This is attributed to the larger steric hindrance of cyclohexene oxide, which hinders the nucleophilic attack of the catalyst and makes it difficult for cyclohexene oxide to open the ring [25, 45]. The above results indicate that MCM-41-N/CH₃(1:3) has the excellent generalization.

3.5 Possible reaction mechanism

Based on the characterization, catalytic reaction results and the previously reported works on the CO₂ cycloaddition reaction by quaternary ammonium ionic liquids [46–52], a feasible reaction mechanism for the CO₂ cycloaddition with PO by MCM-41-N/CH₃(1:3) catalyst was proposed in Fig. 10. The whole cycloaddition process consists of three processes: epoxide ring-opening, CO₂ insertion and ring-closing. In this catalytic system, the Br[−] ions and hydrogen bond donors (hydroxyl groups) synergistically catalyze the reaction. Firstly,

the halogen Br[−] ions in the MCM-41-N/CH₃(1:3) catalyst nucleophilically attack the β-C atoms in the epoxide, and the –OH groups on the MCM-41 molecular sieve activate the oxygen atom in the epoxide through hydrogen bonds, and their synergistic effect causes the epoxide to open the ring, forming the haloalkoxy intermediate. Subsequently, haloalkoxy intermediate interacts with CO₂ to form an alkyl carbonate anion. Finally, an intramolecular ring-closure step by the nucleophilic attack of anionic oxygen atoms towards the carbon atoms bearing bromide achieves the formation of cyclic carbonates and catalyst regeneration.

4 Conclusions

A series of quaternary ammonium ionic liquids functionalized MCM-41 catalysts were successfully prepared using a post-synthetic modification method for catalyzing the CO₂ cycloaddition reaction. The prepared metal-free catalysts can effectively catalyze CO₂ conversion under cocatalyst-free and solvent-free conditions. Among them, the MCM-41-N/CH₃(1:3) catalyst can achieve a yield of 92.5% and selectivity of 96.6% when reacting for 3 h at 2.0 MPa and 140 °C. Moreover, the catalyst can be easily recovered through the simple centrifugation, demonstrating the superior reusability. Additionally, the MCM-41-N/CH₃(1:3) can catalyze CO₂ cycloaddition reactions effectively of various epoxy substrates with excellent substrate compatibility. Furthermore, the MCM-41-N/CH₃(1:3) catalyst exhibits outstanding catalytic properties for the dilute CO₂ conversion to cyclic carbonates. The excellent catalytic performance as well as the confirmed stability make the developed quaternary ammonium ionic liquids MCM-41 hybrid materials a promising heterogeneous catalyst for the CO₂ cycloaddition reaction, and the results of this work will provide some guidance for the development of metal-cocatalyst-solvent-free CO₂ cycloaddition catalysts and ionic liquid functionalized materials.

Table 5 Catalyst properties of MCM-41-N/CH₃(1:3) for the CO₂ cycloaddition with various epoxides substrates

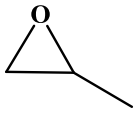
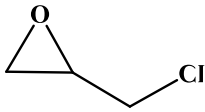
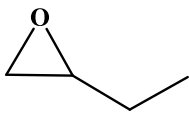
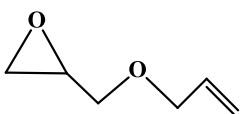
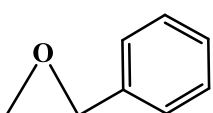

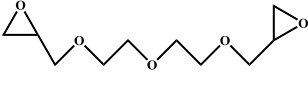

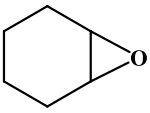
Entry	Epoxides	Yield (%) ^a	Selectivity (%) ^a
1	 PO PO	92.5	96.6
2	 ECH ECH	91.0	94.0
3	 BO BO	91.1	95.5
4	 AGE AGE	90.6	93.5
5	 SO SO	90.0	95.0
6	 BDE BDE	90.6	94.5
7	 DEDG DEDG	90.7	92.4
8	 HDK HDK	90.1	94.3
9	 CO CO	22.9	67.7

Table 5 (continued)

Reaction parameters: epoxy substrates (17 mmol), catalyst addition amount 15 wt%, initial pressure 2.0 MPa, reaction temperature 140 °C, reaction time 3 h

^aDetermined by GC analysis

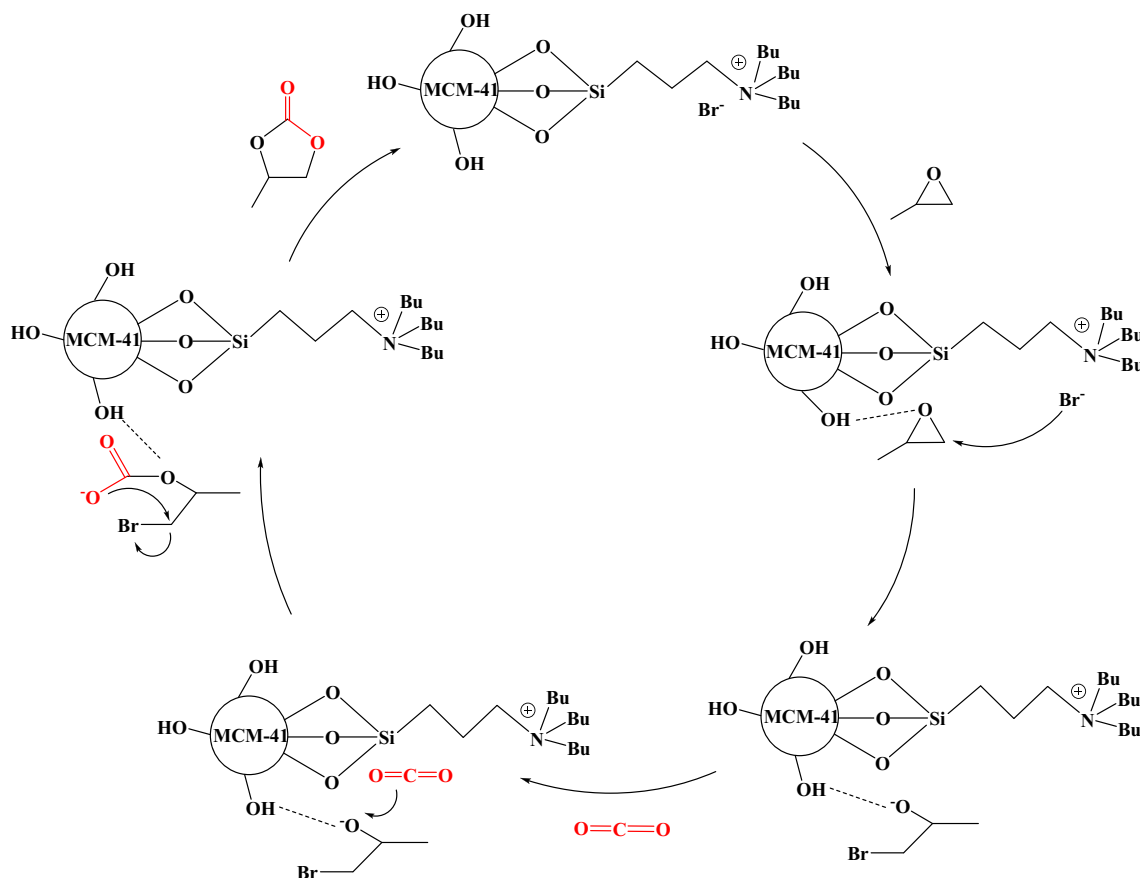


Fig. 10 Feasible mechanism of cycloaddition catalyzed by MCM-41-N/CH₃(1:3)

Acknowledgements The authors acknowledge the financial support provided the Natural Science Foundation of Shandong Province (ZR2021MB135) and the Key Research and Development Plan of Shandong Province (2021ZDSYS13).

Author contributions QL and SW wrote the main manuscript including text, tables and figures. CJ and JD conducted experiments. GC and FG contributed equally with conceptualization and supervision. All authors reviewed the manuscript.

Declarations

Competing interests The authors declare no competing interests.

Research involving human or animal rights This work does not contain any studies with human participants or animals performed by any of the authors.

References

1. A.W. Kleij, M. North, A. Urakawa, CO₂ catalysis. *Chemsuschem* **10**, 1036–1038 (2017). <https://doi.org/10.1002/cssc.201700218>
2. J.L. Wu, X. Liu, R.M. Zhang, J.B. Zhang, H.Y. Si, Z.J. Wu, A novel (CaO/CeO₂)/CeO₂ composite adsorbent based on micro-injection titration-calcination strategy for CO₂ adsorption. *Chem. Eng. J.* **454**, 140485 (2023). <https://doi.org/10.1016/j.cej.2022.140485>
3. W.X. Cao, O. Zhuo, Y.J. Li, B.Z. Yuan, W.H. Luo, Selective adsorption of CO₂/N₂ promoted by polar ligand functional groups of metal–organic frameworks. *J. Porous Mater.* **29**, 63–71 (2022). <https://doi.org/10.1007/s10934-021-01141-w>
4. Z.Q. Yu, M. Shi, Recent advances in the electrochemically mediated chemical transformation of carbon dioxide. *Chem. Commun.* **58**, 13539–13555 (2022). <https://doi.org/10.1039/d2cc05242c>
5. T.K. Pal, D. De, P.K. Bharadwaj, Metal-organic frameworks as heterogeneous catalysts for the chemical conversion of carbon dioxide. *Fuel* **320**, 123904 (2022). <https://doi.org/10.1016/j.fuel.2022.123904>

6. Y.C. Wang, Y.F. Liu, Q. Su, Y.N. Li, L.L. Deng, L. Dong, M.Q. Fu, S.F. Liu, W.G. Cheng, Poly(ionic liquid) materials tailored by carboxyl groups for the gas phase-conversion of epoxide and CO₂ into cyclic carbonates. *J. Carbondioxide Util.* **60**, 101976 (2022). <https://doi.org/10.1016/j.jcou.2022.101976>
7. R. Prajapati, N. Tsunoji, M. Bandyopadhyay, R. Bandyopadhyay, Hierarchical, amine functionalized silicoaluminophosphate molecular sieves for the synthesis of cyclic carbonate via CO₂ utilization. *J. Porous Mater.* **30**, 2087–2099 (2023). <https://doi.org/10.1007/s10934-023-01488-2>
8. N. Laiwattanapaisarn, A. Virachotikul, K. Phomphrai, Cycloaddition of carbon dioxide to epoxides by highly active constrained aluminum chloride complexes. *Dalton Trans.* **50**, 11039–11048 (2021). <https://doi.org/10.1039/D1DT01903A>
9. Y.M. Shen, W.L. Duan, M. Shi, Phenol and organic bases co-catalyzed chemical fixation of carbon dioxide with terminal epoxides to form cyclic carbonates. *Adv. Synth. Catal.* **345**, 337–340 (2003). <https://doi.org/10.1002/adsc.200390035>
10. Q.Y. Yuan, P. Zhang, Y.L. Shi, D.H. Liu, Dual-ligand complex catalysts for the cycloaddition of propylene oxide and carbon dioxide. *J. Mol. Struct.* **1150**, 329–334 (2017). <https://doi.org/10.1016/j.molstruc.2017.08.056>
11. Y. Chen, Y.J. Li, H. Wang, Z.F. Chen, Y.Z. Lei, Int. Facile construction of carboxyl-functionalized ionic polymer towards synergistic catalytic cycloaddition of carbon dioxide into cyclic carbonates. *J. Mol. Sci.* **23**, 10879 (2022). <https://doi.org/10.3390/ijms231810879>
12. Y.T. Tong, R.H. Cheng, H. Dong, B.P. Liu, Efficient cycloaddition of CO₂ and epoxides to cyclic carbonates using salen-based covalent organic framework as a heterogeneous catalyst. *J. Porous Mater.* **29**, 1253–1263 (2022). <https://doi.org/10.1007/s10934-022-01246-w>
13. J. Tapiador, E. García-Rojas, P. Leo, C. Martos, G. Calleja, G. Orcajo, Copper MOFs performance in the cycloaddition reaction of CO₂ and epoxides. *Microporous Mesoporous Mater.* **361**, 112741 (2023). <https://doi.org/10.1016/j.micromeso.2023.112741>
14. X. Fang, L. Yang, Z.B. Dai, D. Cong, D.Y. Zheng, T. Yu, R. Tu, S.L. Zhai, J.X. Yang, F.L. Song, H. Wu, W.Q. Deng, C.C. Liu, Poly(ionic liquid)s for photo-driven CO₂ cycloaddition: electron donor–acceptor segments matter. *Adv. Sci.* **10**, 2206687 (2023). <https://doi.org/10.1002/advs.202206687>
15. M. Smiglak, J.M. Pringle, X. Lu, L. Han, S. Zhang, H. Gao, D.R. MacFarlane, R.D. Rogers, Ionic liquids for energy, materials, and medicine. *Chem. Commun.* **50**, 9228–9250 (2014). <https://doi.org/10.1039/C4CC02021A>
16. V.B. Saptal, B.M. Bhanage, Current advances in heterogeneous catalysts for the synthesis of cyclic carbonates from carbon dioxide. *Curr. Opin. Green Sust.* **3**, 1–10 (2017). <https://doi.org/10.1016/j.cogsc.2016.10.006>
17. D.N. Zheng, P. Ning, J.M. Jiang, F. Liu, L. Wang, J.L. Zhang, Effect of ionic liquids clusters microenvironment on cycloaddition reaction of carbon dioxide. *J. Mol. Liq.* **284**, 68–74 (2019). <https://doi.org/10.1016/j.molliq.2019.03.165>
18. S.H. Lian, C.F. Song, Q.L. Liu, E.H. Duan, H.W. Ren, Y. Kitamura, Recent advances in ionic liquids-based hybrid processes for CO₂ capture and utilization. *J. Environ. Sci.* **99**, 281–295 (2021). <https://doi.org/10.1016/j.jes.2020.06.034>
19. W.L. Dai, B. Jin, S.L. Luo, X.B. Luo, X.M. Tu, C.T. Au, Functionalized phosphonium-based ionic liquids as efficient catalysts for the synthesis of cyclic carbonate from epoxides and carbon dioxide. *Appl. Catal. A* **470**, 183–188 (2014). <https://doi.org/10.1016/j.apcata.2013.10.060>
20. D.Y. Kim, S. Subramanian, D. Thirion, Y. Songa, A. Jamal, M.S. Otaib, C.T. Yavuz, Quaternary ammonium salt grafted nanoporous covalent organic polymer for atmospheric CO₂ fixation and cyclic carbonate formation. *Catal. Today* **356**, 527–534 (2020). <https://doi.org/10.1016/j.cattod.2020.03.050>
21. B.F. Goodrich, J.C. Delafuente, B.E. Gurkan, D.J. Zadigian, E.A. Price, Y. Huang, J.F. Brennecke, Experimental measurements of amine-functionalized anion-tethered ionic liquids with carbon dioxide. *Ind. Eng. Chem. Res.* **50**, 111–118 (2011). <https://doi.org/10.1021/ie101688a>
22. Y.L. Wan, L. Wang, L.L. Wen, Amide-functionalized organic cationic polymers toward enhanced catalytic performance for conversion of CO₂ into cyclic carbonates. *J. Carbondioxide Util.* **64**, 102174 (2022). <https://doi.org/10.1016/j.jcou.2022.102174>
23. J. Peng, S. Wang, H.J. Yang, B.R. Ban, Z.D. Wei, L.H. Wang, B. Lei, Highly efficient fixation of carbon dioxide to cyclic carbonates with new multi-hydroxyl bis-(quaternary ammonium) ionic liquids as metal-free catalysts under mild conditions. *Fuel* **224**, 481–488 (2018). <https://doi.org/10.1016/j.fuel.2018.03.119>
24. D. Jadav, D.K. Pandey, T. Patil, D.K. Singh, S. Dharaskar, R. Bandyopadhyay, N. Tsunoji, R. Kumar, M. Bandyopadhyay, Ordered silica matrices supported ionic liquids as highly efficient catalysts for fine chemical synthesis. *J. Porous Mater.* **29**, 2003–2017 (2022). <https://doi.org/10.1007/s10934-022-01312-3>
25. Q. Li, W.L. Da, J. Mao, X.W. He, Y. Liu, Y. Xu, L.X. Yang, J.P. Zou, X.B. Luo, Facile integration of hydroxyl ionic liquid into Cr-MIL-101 as multifunctional heterogeneous catalyst for promoting the efficiency of CO₂ conversion. *Microporous Mesoporous Mater.* **350**, 112461 (2023). <https://doi.org/10.1016/j.micromeso.2023.112461>
26. Y. Wang, R.F. He, C. Wang, G. Li, Ionic liquids supported at MCM-41 for catalyzing CO₂ into cyclic carbonates without co-catalyst. *React. Kinet. Mech. Catal.* **134**, 823–835 (2021). <https://doi.org/10.1007/s11144-021-02097-3>
27. F. Adam, J.N. Appaturi, E.P. Ng, Halide aided synergistic ring opening mechanism of epoxides and their cycloaddition to CO₂ using MCM-41-imidazolium bromide catalyst. *J. Mol. Catal. A* **386**, 42–48 (2014). <https://doi.org/10.1016/j.molcata.2014.02.008>
28. S. Udayakumar, S.W. Park, D.W. Park, B.S. Choi, Immobilization of ionic liquid on hybrid MCM-41 system for the chemical fixation of carbon dioxide on cyclic carbonate. *Catal. Commun.* **9**, 1563–1570 (2008). <https://doi.org/10.1016/j.catcom.2008.01.001>
29. A. Rehman, F. Saleem, F. Javed, A. Ikhlaiq, S.W. Ahmad, A. Harvey, Recent advances in the synthesis of cyclic carbonates via CO₂ cycloaddition to epoxides. *J. Environ. Chem. Eng.* **9**, 105113 (2021). <https://doi.org/10.1016/j.jece.2021.105113>
30. W.G. Cheng, B.N. Xiao, J. Sun, K. Dong, P. Zhang, S.J. Zhang, F.T.T. Ng, Effect of hydrogen bond of hydroxyl-functionalized ammonium ionic liquids on cycloaddition of CO₂. *Tetrahedron Lett.* **56**, 1416–1419 (2015). <https://doi.org/10.1016/j.tetlet.2015.01.174>
31. S. Yue, H.L. Qu, X.X. Song, X.N. Feng, Novel hydroxyl-functionalized ionic liquids as efficient catalysts for the conversion of CO₂ into cyclic carbonates under metal/halogen/cocatalyst/solvent-free conditions. *New J. Chem.* **46**, 5881–5888 (2022). <https://doi.org/10.1039/D2NJ00257D>
32. A. Jentys, K. Kleestorfer, H. Vinek, Concentration of surface hydroxyl groups on MCM-41. *Microporous Mesoporous Mater.* **27**, 321–328 (1999). [https://doi.org/10.1016/S1387-1811\(98\)00265-0](https://doi.org/10.1016/S1387-1811(98)00265-0)
33. H. Chen, S.Y. Dong, Y.J. Zhang, P.Y. He, A comparative study on energy efficient CO₂ capture using amine grafted solid sorbent: materials characterization, isotherms, kinetics and thermodynamics. *Energy* **239**, 122348 (2022). <https://doi.org/10.1016/j.energy.2021.122348>
34. L. Muniandy, F. Adam, N.R.A. Rahman, E.P. Ng, Highly selective synthesis of cyclic carbonates via solvent free cycloaddition of CO₂ and epoxides using ionic liquid grafted on rice husk derived

- MCM-41. *Inorg. Chem. Commun.* **104**, 1–7 (2019). <https://doi.org/10.1016/j.inoche.2019.03.012>
35. X.W. Zhang, Y.Y. Huang, J. Yang, H.X. Gao, Y.Q. Huang, X. Luo, Z.W. Liang, P. Tontiwachwuthikul, Amine-based CO₂ capture aided by acid-basic bifunctional catalyst: advancement of amine regeneration using metal modified MCM-41. *Chem. Eng. J.* **383**, 123077 (2020). <https://doi.org/10.1016/j.cej.2019.123077>
36. S. Sharma, U.P. Singh, A.P. Singh, Synthesis of MCM-41 supported cobalt (II) complex for the formation of polyhydroquinoline derivatives. *Polyhedron* **199**, 115102 (2021). <https://doi.org/10.1016/j.poly.2021.115102>
37. F. Adam, M.S. Batagarawa, Tetramethylguanidine-silica nanoparticles as an efficient and reusable catalyst for the synthesis of cyclic propylene carbonate from carbon dioxide and propylene oxide. *Appl. Catal. A* **454**, 164–171 (2013). <https://doi.org/10.1016/j.apcata.2012.12.009>
38. M. Kida, Y. Jin, J. Nagao, Changes in the ¹³C NMR spectra of tetra-n-butylammonium chloride by clathrate hydration. *Chem. Phys.* **522**, 233–237 (2019). <https://doi.org/10.1016/j.chemphys.2019.03.010>
39. R.J. Ramalingam, J.N. Appaturi, T. Pulingam, N. Ibrahim, H.A. Al-Lohedan, Synthesis, characterization and catalytic activity of ionic liquid mimic halides modified MCM-41 for solvent free synthesis of phenyl glycidyl carbonate. *Mater. Chem. Phys.* **233**, 79–88 (2019). <https://doi.org/10.1016/j.matchemphys.2019.05.045>
40. S. Udayakumar, M.-K. Lee, H.-L. Shim, S.-W. Park, D.-W. Park, Imidazolium derivatives functionalized MCM-41 for catalytic conversion of carbon dioxide to cyclic carbonate. *Catal. Commun.* **10**, 659–664 (2009). <https://doi.org/10.1016/j.catcom.2008.11.017>
41. W.L. Dai, P. Mao, Y. Liu, S.Q. Zhang, B. Li, L.X. Yang, X.B. Luo, J.P. Zou, Quaternary phosphonium salt-functionalized Cr-MIL-101: A bifunctional and efficient catalyst for CO₂ cycloaddition with epoxides. *J. Carbon Dioxide Util.* **36**, 295–305 (2020). <https://doi.org/10.1016/j.jcou.2019.10.021>
42. J.N. Appaturi, F. Adam, A facile and efficient synthesis of styrene carbonate via cycloaddition of CO₂ to styrene oxide over ordered mesoporous MCM-41-Imi/Br catalyst. *Appl. Catal. B* **136–137**, 150–159 (2013). <https://doi.org/10.1016/j.apcatb.2013.01.049>
43. F. Jutz, A. Buchard, M.R. Kember, S.B. Fredriksen, C.K. Williams, Mechanistic investigation and reaction kinetics of the low-pressure copolymerization of cyclohexene oxide and carbon dioxide catalyzed by a dizinc complex. *J. Am. Chem. Soc.* **133**, 17395–17405 (2011). <https://doi.org/10.1021/ja206352x>
44. L.Y. Zhao, N. Liu, H. Huang, X.F. Wang, X.L. Huang, Synthesis of propylene carbonate from carbon dioxide through high activity of magnesium oxide. *J. Chem. Eng. Jpn.* **52**, 406–412 (2019). <https://doi.org/10.1252/jcej.18we073>
45. T. Chang, X.L. Yan, Y. Li, Y.J. Hao, X.Y. Fu, X.H. Liu, B. Panchal, S.J. Qin, Z. Zhu, Quaternary ammonium immobilized PAMAM as efficient catalysts for conversion of carbon dioxide. *J. Carbon Dioxide Util.* **58**, 101913 (2022). <https://doi.org/10.1016/j.jcou.2022.101913>
46. Y. Qu, Y.F. Zhao, D.Z. Li, J.M. Sun, Task-specific ionic liquids for carbon dioxide absorption and conversion into value-added products. *Curr. Opin. Green Sust.* **34**, 100599 (2022). <https://doi.org/10.1016/j.cogsc.2022.100599>
47. M.S. Liu, X. Wang, Y.C. Jiang, J.M. Sun, M. Arai, Hydrogen bond activation strategy for cyclic carbonates synthesis from epoxides and CO₂: current state-of-the-art of catalyst development and reaction analysis. *Catal. Rev.* **61**, 214 (2019). <https://doi.org/10.1080/01614940.2018.1550243>
48. M. North, R. Pasquale, C. Young, Synthesis of cyclic carbonates from epoxides and CO₂. *Green Chem.* **12**, 1514–1539 (2010). <https://doi.org/10.1039/C0GC00065E>
49. V. Caló, A. Nacci, A. Monopoli, A. Fanizzi, Cyclic carbonate formation from carbon dioxide and oxiranes in tetrabutylammonium halides as solvents and catalysts. *Org. Lett.* **4**, 2561–2563 (2002). <https://doi.org/10.1021/ol026189w>
50. D.H. Lan, Y.X. Gong, N.Y. Tan, S.S. Wu, J. Shen, K.C. Yao, B. Yi, C.T. Au, S.F. Yin, Multi-functionalization of GO with multi-cationic ILs as high efficient metal-free catalyst for CO₂ cycloaddition under mild conditions. *Carbon* **127**, 245–254 (2018). <https://doi.org/10.1016/j.carbon.2017.11.007>
51. J. Sun, S.J. Zhang, W.G. Cheng, J.Y. Ren, Hydroxyl-functionalized ionic liquid: a novel efficient catalyst for chemical fixation of CO₂ to cyclic carbonate. *Tetrahedron Lett.* **49**, 3588–3591 (2008). <https://doi.org/10.1016/j.tetlet.2008.04.022>
52. L.Q. Xiao, Y.M. Lai, R. Zhao, Q.Y. Song, J.Y. Cai, X.Y. Yin, Y.L. Zhao, L.X. Hou, Ionic conjugated polymers as heterogeneous catalysts for the cycloaddition of carbon dioxide to epoxides to form carbonates under solvent- and cocatalyst-free conditions. *ChemPlusChem* **87**, e202200324 (2022). <https://doi.org/10.1002/cplu.202200324>

Publisher's Note Springer Nature remains neutral with regard to jurisdictional claims in published maps and institutional affiliations.

Springer Nature or its licensor (e.g. a society or other partner) holds exclusive rights to this article under a publishing agreement with the author(s) or other rightsholder(s); author self-archiving of the accepted manuscript version of this article is solely governed by the terms of such publishing agreement and applicable law.